

Synergistic signatures of group mechanisms in higher-order systems

Thomas Robiglio,^{1,*} Matteo Neri,² Davide Coppes,³ Cosimo Agostinelli,³
 Federico Battiston,¹ Maxime Lucas,^{4,†} and Giovanni Petri^{5,4,6,‡}

¹*Department of Network and Data Science, Central European University, Vienna, Austria*

²*Institut de Neurosciences de la Timone, Aix Marseille Université, Marseille, France*

³*Department of Physics, University of Turin, Turin, Italy*

⁴*CENTAI Institute, Turin, Italy*

⁵*NPLab, Network Science Institute, Northeastern University London, London, UK*

⁶*Networks Unit, IMT Lucca, Lucca, Italy*

(Dated: January 23, 2024)

The interplay between causal mechanisms and emerging collective behaviors is a central aspect of the understanding, control, and prediction of complex networked systems. Here we study this interplay in the context of higher-order mechanisms and behaviors in two representative models: a simplicial Ising model and a simplicial social contagion model. In both systems, we find that group (higher-order) interactions show emergent synergistic (higher-order) behavior. The emergent synergy appears only at the group level and depends in a complex non-linear way on the tradeoff between the strengths of the low- and higher-order mechanisms, and is invisible to low-order behavioral observables. Finally, we present a simple method to detect higher-order mechanisms by using this signature.

Mechanisms and behaviors are two facets of the study of complex systems: *mechanisms* are the structural and dynamical rules that control the causal evolution of the system; *behaviors*, instead, refer to the measurable observables that quantify statistical interdependencies between units of a system in space and time (Fig. 1). The nature of the relation between the two facets and the limits of our capacity to reconstruct it is a long-standing problem in complex interacting systems [1–7].

Existing methods to study each of the two facets mostly adopt pairwise (lower-order) descriptions: pairwise network representations for mechanisms [8, 9], and low-order information-theoretic metrics for behaviors [10–12]. However, despite their success, these low-order methods often fail to fully capture the intricate nuances inherent to many complex systems [13, 14], and non-pairwise (also called polyadic, or higher-order) methods are being developed: higher-order network representations such as hypergraph or simplicial complexes [15] and higher-order behavioral metrics, both topological [16] and information-theoretic [17, 18].

In this context, a central question is then: *what is the relation between higher-order mechanisms and behaviors?* Intuition would suggest that observing higher-order behaviors implies the presence of higher-order mechanisms. However, this is not the case: early results show that systems with only low-order mechanisms can display non-trivial higher-order behaviors [19], and—conversely—higher-order mechanisms can lead to low-order behaviors [14]. Thus, a systematic investigation of this complex relation is needed.

Toward this goal, here we thoroughly explore the mechanism-behaviors relation in higher-order versions of two canonical dynamical processes—an Ising model [20, 21] that we introduce, and an existing social contagion

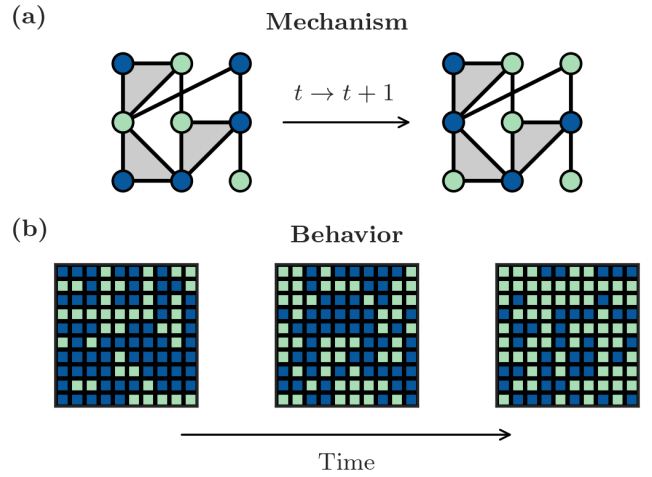


FIG. 1. **Mechanisms versus behaviors in complex systems.** (a) Mechanisms consists of (i) the topological structure of interactions between nodes, and (ii) the rules controlling the temporal evolution of the states of the nodes. (b) Behaviors are the observable states of the system and encompass its spatial and temporal patterns, interdependencies between units, and emergent phenomena. In experimental data, behaviors are often the only available.

model [22]—and quantify higher-order behavior by defining the *total dynamical O-information*, an extension of the transfer entropy to groups of variables of arbitrary size [17, 23]. In both systems, we uncover an emergent synergistic behavioral signature of group interactions. Synergistic behavior manifests when information about a group of variables can only be recovered by considering the joint state of all variables, and cannot be reconstructed from subsets of units of the group. Crucially, the observed behavioral signatures display a complex non-linear dependence on the strength of the pa-

parameter controlling the higher-order mechanisms. While these signatures can in some regimes be overshadowed by other emergent phenomena in the systems (*e.g.* the transition to the magnetized phase in the Ising model), when present, they are invisible to low-order observables, and thus represent genuine higher-order phenomena. Finally, we present a simple method leveraging the emergent synergies for the explicit detection of higher-order mechanisms.

Quantifying higher-order behaviors. The partial information decomposition (PID) framework is a well-established approach to characterize the information-sharing interdependencies between three or more variables [24–26]. Qualitatively, these relations can be of three types: redundant, synergistic, or unique. Consider three variables sharing information, X_1 , X_2 and X_3 . Information is said to be redundant if it is replicated over the variables (that is, recoverable from $X_1 \vee X_2 \vee X_3$), synergistic if it can only be recovered from their joint state ($X_1 \wedge X_2 \wedge X_3$), and unique if it can only be recovered from one variable and nowhere else. In this framework, mutual information has been extended to groups of three or more variables by the so-called O-information Ω [17]. To generalize the O-information of multivariate time series from equal-time correlations to time-lagged correlations—similarly to how transfer entropy extends mutual information [27]—Stramaglia *et al.* proposed *dynamical* O-information $d\Omega$ [23]. This quantity is defined by (i) considering n random variables $\mathbf{X} = (X_1, \dots, X_n)$ on which we compute the standard O-information $\Omega_n(\mathbf{X})$, (ii) adding a new random variable Y , and (iii) computing the variation of O-information: $\Delta_n = \Omega_{n+1}(\mathbf{X}, Y) - \Omega_n(\mathbf{X})$. To remove potentially confounding shared information due to common history or input signals, the dynamical O-information is defined by conditioning Δ_n on the history Y_0 of the target variable Y :

$$d\Omega_n(Y; \mathbf{X}) \equiv (1 - n) \mathcal{I}(Y; \mathbf{X} | Y_0) + \sum_{j=1}^n \mathcal{I}(Y; \mathbf{X}_{-j} | Y_0). \quad (1)$$

Here, $\mathcal{I}(\cdot; \cdot | \cdot)$ is the conditional mutual information, $Y_0(t) = (y(t), y(t-1), \dots, y(t-\tau+1))$ is the past and present of Y , and $Y = Y(t) = y(t+1)$ its next instance. The parameter τ is the temporal horizon of the time series and can typically be set to a relevant time scale of the process. To quantify the dynamical information within a group of n units, regardless of source-target assignments, we define the *total* (or symmetrized) dynamical O-information as:

$$d\Omega_n^{\text{tot.}}(\mathbf{X}) \equiv \sum_{j=1}^n d\Omega_{n-1}(X_j; \mathbf{X}_{-j}). \quad (2)$$

Total dynamical O-information inherits from O-information the property of being a signed metric:

$d\Omega_n^{\text{tot.}}(\mathbf{X}) > 0$ indicates that information-sharing among the units of \mathbf{X} is dominated by redundancy, $d\Omega_n^{\text{tot.}}(\mathbf{X}) < 0$ indicates that it is dominated by synergy, and $d\Omega_n^{\text{tot.}}(\mathbf{X}) = 0$ indicates a balance between both.

Dynamical systems with higher-order mechanisms. We consider two dynamical models with higher-order interactions: a simplicial Ising model and the simplicial model of social contagion [22]. Both are defined on simplicial complexes, a particular class of hypergraphs [15] that encode multi-node interactions as simplices and respect downward closure—for any simplex in the simplicial complex, all its sub-simplices must be included too.

The first discrete dynamical system we consider is a simplicial Ising model. This model is an extension of the standard Ising model [20, 21] that includes group interactions of different strengths for simplices of different sizes. We consider a simplicial complex \mathcal{K} with average generalized degrees $\{\langle k_\ell \rangle\}$, where each of the N nodes has two possible states: spin-up ($S^i = +1$) or spin-down ($S^i = -1$). The model is defined by the Hamiltonian:

$$H = -J_0 \sum_{i=1}^N S^i + \sum_{\ell=1}^{\ell_{\max}} \frac{J_\ell}{\langle k_\ell \rangle} \sum_{\{\sigma \in \mathcal{K}: |\sigma|=\ell\}} \left[2 \bigotimes_{i \in \sigma} S^i - 1 \right] \quad (3)$$

where ℓ_{\max} is the maximal order of \mathcal{K} and:

$$\bigotimes_{i=1}^n S^i = \delta(S^1, \dots, S^n) = \begin{cases} 1 & \text{if } S^1 = \dots = S^n \\ 0 & \text{otherwise} \end{cases} \quad (4)$$

is the Kronecker delta with an arbitrary number of binary arguments. For $\ell_{\max} = 1$, *i.e.* structures with only pairwise interactions, the model reduces to the standard Ising model with a uniform magnetic field J_0 and two-body coupling strength J_1 . The introduction of the Kronecker delta—instead of the usual product [28–30]—in the coupling terms is necessary to preserve the parity symmetry under spin flip at all sites of the dyadic model without magnetic field ($J_0 = 0$). We consider the dynamics of this system to be the Markov chain of Monte Carlo moves performed with the Metropolis-Hastings acceptance-rejection rule [31] at temperature T .

The second discrete dynamical model that we consider is the simplicial model of social contagion [22]. Following the SIS framework [32], we associate with each of the N nodes of a simplicial complex \mathcal{K} a binary random variable $x_i(t) \in \{0, 1\}$. At each time step we divide the population of individuals into two classes of susceptible (S) and infectious (I) nodes, corresponding, respectively, to the values 0 and 1 of the state variables $x_i(t)$. At the initial time step t_0 , a finite fraction of infected agents $\rho_0 = \sum_i x_i(t_0)/N$ is placed in the population. At each time step, each susceptible agent ($x_i(t) = 0$) becomes infected with a probability β_ℓ if it belongs to a ℓ -simplex

where all other ℓ nodes are infected. Infected agents recover independently with probability μ . As is customary, we introduce the rescaled infectivity parameter of order ℓ : $\lambda_\ell = \beta_\ell \langle k_\ell \rangle / \mu$, where k_ℓ is the generalized degree of order ℓ .

For computational feasibility, in the following, we limit ourselves to group mechanisms (interactions) and interdependencies of up to three nodes, that is, $\ell_{\max} = 2$. Unless stated otherwise, the results shown are obtained in a random simplicial complex with $N = 200$ nodes and average degrees $\langle k_1 \rangle = 20$, $\langle k_2 \rangle = 6$. The Ising model was simulated for 3×10^4 time steps, and the contagion model for 10^4 time steps. Other parameters were set to $T = 1$ (Ising) and $\mu = 0.8$ and $\rho_0 = 0.3$ (social contagion).

Emergence of synergistic signatures of group interactions. We simulate the two dynamical systems for different values of the control parameters and compute the total dynamical O-information $d\Omega_3^{\text{tot.}}$ on the resulting time series for different *types* of groups of three nodes: 2-simplices, 3-cliques, and uniformly randomly chosen triplets of nodes not part of the previous two groups. In both cases, we set the delay $\tau = 1$ as both systems are Markovian. As we increase the strength of group interactions (J_2 , the three-body coupling in the Ising model, and λ_2 , the group rescaled infection rate in the contagion model), we observe an increasing co-occurrence of higher-order mechanisms and synergistic higher-order behaviors (Fig. 2). In both systems, we see that all types of groups of three nodes display synergistic higher-order behaviors ($d\Omega_3^{\text{tot.}} < 0$); however, and crucially, as we increase the relative strength of the higher-order mechanisms (J_2 and λ_2), we see that 2-simplices, *i.e.* the genuine higher-order interactions, display significantly stronger synergistic behaviors than the other groups of three nodes.

Insufficiency of lower-order metrics. Although we showed the presence of strong synergistic behaviors in the presence of genuine higher-order interactions, we still do not know the extent of this correspondence, nor whether low-order observables could already detect—and to what degree—the presence of higher-order interactions. Moreover, we need to determine whether the group behaviors are truly higher-order or just the byproduct of low-order interdependencies. To answer these questions, we compare our higher-order metric (total dynamical O-information) with a lower-order information metric, over the parameter space of both systems. For the lower-order metric, for each group of three nodes, we compute the sum Σ of the transfer entropies between the time series of the three possible node pairs. For each of these metrics, we then quantify the difference in behavior between 2-simplices and 3-cliques (that is, lower- and higher-order mechanisms, respectively) in terms of the statistical distance [33]. The statistical distance (or total variation distance) d [34] between two distributions—here, P_2 for 2-simplices and P_3 for 3-cliques—over a common alpha-

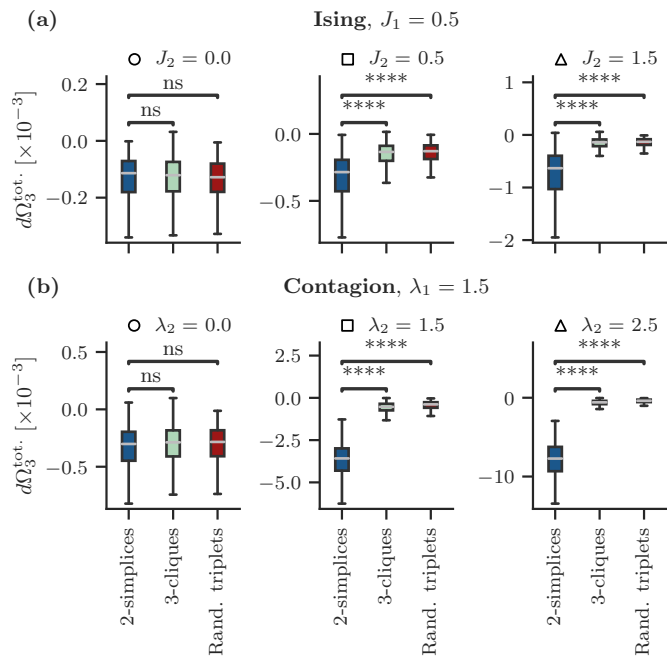


FIG. 2. **Synergistic signature of higher-order mechanisms.** We show box plots of the distributions of total dynamical O-info $d\Omega_3^{\text{tot.}}$ in (a) the simplicial Ising, and (b) the simplicial contagion models. Distributions are over all occurrences of three types of motifs in the simplicial complex: 2-simplices (blue), 3-cliques (green), and random triplets (red), and are shown for increasing values of the group mechanism strengths (J_2 and λ_2). As strength increases, higher-order interactions become more synergistic (negative $d\Omega_3^{\text{tot.}}$) than lower ones. Symbols “ns” and “****” indicate a non-significant and significant ($p \leq 10^{-4}$) difference, respectively, between the distributions (t -test).

bet χ , is defined as:

$$d(P_2, P_3) = \frac{1}{2} \sum_{x \in \chi} |P_2(x) - P_3(x)|, \quad (5)$$

which we denote $d_{23} \equiv d(P_2, P_3)$ for short. Distance d_{23} quantifies the overlap and similarity of the two distributions. By definition, it takes values in $[0, 1]$: $d_{23} = 0$ if the two distributions are identical, and $d_{23} = 1$ if the two distributions take non-zero values on non-overlapping subsets of χ [35].

We find two main results—valid for both systems—about the relation between higher-order behaviors and mechanisms. First, we see that the low-order behavioral metric does not see much difference between the lower- (3-cliques) and higher-order mechanisms (2-simplices) whereas the higher-order metric does. Indeed, this is indicated by the uniformly low values of d_{23} with low-order metric Σ (Fig. 3a,c) with respect to the large values exhibited by d_{23} with the higher-order metric, the total dynamical O-information (Fig. 3b,d). The latter is consistent with the synergetic signature results shown in Fig. 2. So, the higher-order mechanisms can be identified—and distinguished from low-order mechanisms—by the

higher-order behavioral metric but not by the low-order one.

Second, focusing on the higher-order behavioral metric $d\Omega_3^{\text{tot}}$, we see that the difference between the 2-simplices and 3-cliques is large (large d_{23} , dark blue) over a finite region of parameter space (Fig. 3b,d). This region corresponds to the co-occurrence of higher-order mechanisms and synergistic higher-order behavior (as shown in Fig. 2). We see that it occurs for sufficiently large values of the strength of the higher-order mechanisms (J_2 and λ_2).

The above observations are common to both models, but each model also has its own specificities. Although fully explaining the shape of the dark blue region is a hard task, we here describe it and explain some of its features. In the Ising model (Fig. 3b), the large $d_{23} \gtrsim 0.5$ region (dark blue) does not extend above $J_1^{\text{cr}} = 1$ (dashed line), which is the magnetization threshold of the pairwise model with no magnetic field [36]. This can be understood because, above that value, the system is magnetized and no information can be recovered as the system is frozen in the configuration with minimal energy. Below the threshold ($J_1 < 1$), the region appears above a certain strength of the three-body coupling $J_2 \gtrsim 0.5$, and that value seems to decrease as J_1 increases.

In the contagion model (Fig. 3d) the large d_{23} region displays larger values ($0.7 \lesssim d_{23} \lesssim 1.0$). It does not appear to be bounded from above, contrary to that of the Ising model. However, it is bounded from below. First, for $\lambda_1 < 1$ (left of the vertical dashed line), the region appears only above $\lambda_{\text{cr}} = 2\sqrt{\lambda_2} - \lambda_2$ (dashed-dotted line). These values are known: $\lambda_1 = 1$ is the epidemic threshold of the pairwise version of the model (SIS) and λ_{cr} is the value where the discontinuous transition occurs [22]. This makes sense: below that value, only the epidemic-free state exists, for which we do not expect to see higher-order behaviors. Second, the region does not appear to extend below $\lambda_2 = 1$ (horizontal dashed line), below which we know that no discontinuous transition can exist, and we thus expect the system to behave more like its low-order variant (SIS). Finally, for larger λ_1 , the region starts above values of λ_2 that are larger as λ_1 increases, suggesting that their ratio plays a role.

Synergy-based detection of higher-order interactions. It is possible to exploit the relation between higher-order mechanisms and behaviors to detect higher-order interactions from dynamic. We set ourselves in the case in which we want to discriminate between true higher-order interactions (2-simplices) and spurious ones (3-cliques) having access to the nodes' states' time series, the low-order structure of the system and its average generalized degree of order $\ell = 2$. This setup reproduces the situation in which we have access to the node-level activity of a system, its pairwise structure, and some very coarse information about nodes' neighborhoods in terms of their higher-order connectivity (*e.g.* through local samples).

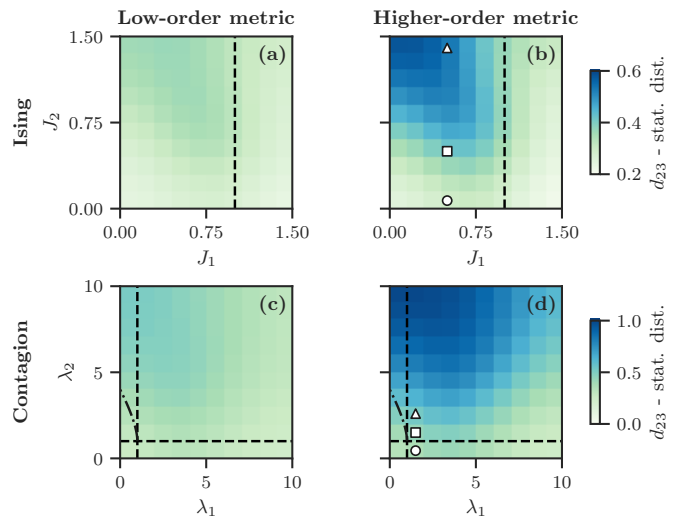


FIG. 3. Low-order metrics do not see the synergistic signature of higher-order mechanisms. We show the statistical distance d_{23} between the distributions of behavior of 2-simplices and 3-cliques, for two metrics: (a), (c) sum of transfer entropies Σ (low-order) and (b), (d) total dynamical O-information (higher-order). Two models are shown. (a), (b) The simplicial Ising model, where the dashed line is the critical coupling strength of the pairwise model $J_1^{\text{cr}} = 1$ with no magnetic field. (c), (d) The simplicial contagion model, where the two dashed lines are, respectively, the epidemic threshold of the pairwise SIS model $\lambda_1^{\text{cr}} = 1$ and the critical value of the rescaled 2-simplices infectivity rate above which the system shows the discontinuous phase transition and bistability $\lambda_2^{\text{cr}} = 1$, and the dash-dotted line represents the points (λ_1, λ_2) where the system undergoes a discontinuous transition [22]. The three white symbols in (b) and (d) correspond to the parameter values showed in Fig. 2.

The heuristic method for the detection of higher-order interactions is simple. Given the average generalized degree $\langle k_2 \rangle$ and the number of nodes, we can compute the expected number of 2-simplices in the system as a simple $n_{\Delta} = N \langle k_2 \rangle / 3$. Once the expected number of 2-simplices within the system is computed we compute the total dynamical O-information for all groups of three nodes connected by pairwise connections (*i.e.* the 3-cliques in the skeleton of the simplicial complex \mathcal{K} under study), rank them by their values of $d\Omega_3^{\text{tot}}$ and mark as “predicted” higher-order interactions the n_{Δ} most synergistic ones.

The results of our simple method for the detection of higher-order interactions are shown in Fig. 4 in terms of accuracy scores (fraction of true positives). These results retrace what was already observed with the statistical distance in the higher-order behavior between 2-simplices and 3-cliques. The higher-order behavior is more evident in the simplicial contagion model, allowing for accuracy scores of up to ~ 0.9 , than in the Ising model, accuracy scores only up to ~ 0.7 , in the region in which we observe the synergistic signature this is always significantly better than the random choice accuracy of 0.3 (see SM). We also observe a complex non-linear dependence of the

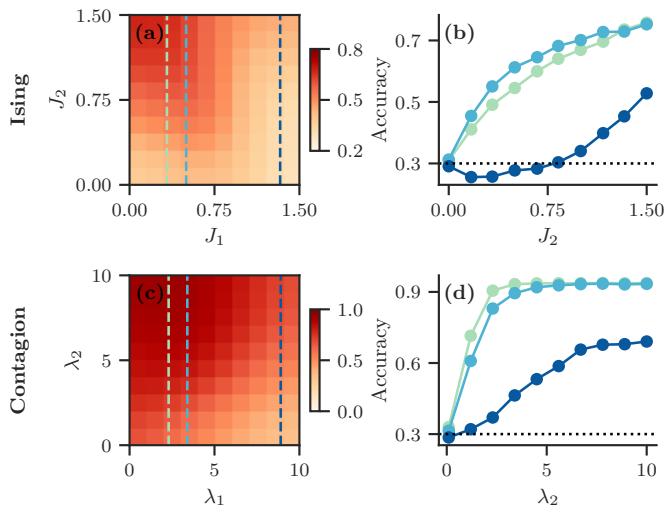


FIG. 4. **Detection of higher-order interactions using higher-order synergistic behavior.** We show the accuracy (fraction of true positives) of the detection of higher-order interactions for (a)-(b) the Ising and (c)-(d) the simplicial contagion models. (a), (c) Full parameter space, and (b), (d) show three example curves corresponding to the dashed lines in (a) and (c). The dotted lines in (b) and (d) indicate the accuracy of the random choice.

accuracy score on the strength of the parameter controlling the higher-order mechanisms (Fig. 4b,d). This complex dependency is a byproduct of the non-linear response of higher-order behaviors ($d\Omega_3^{\text{tot}}$) to the variation of higher-order mechanisms (see SM). This detection method can be applied to more general set-ups (*e.g.* detecting group interactions among all possible combinations of three nodes) leading to similar results.

In conclusion, by exploring the relation between mechanisms and behaviors in two dynamical systems with higher-order interactions, we uncovered emergent synergistic signatures characterizing group mechanisms. Quantifying higher-order behaviors using $d\Omega_3^{\text{tot}}$, we showed that in both models an increase in the relative strength of the parameter controlling the group mechanisms in 2-simplices led (non-linearly) to significantly larger synergistic values of $d\Omega_3^{\text{tot}}$. Crucially, low-order observables (transfer entropy) were not able to capture these signatures, supporting the importance of higher-order observables to study group interdependencies that are irreducible to combinations of low-order ones. By exploring the space of the control parameters of the two systems under study, we showed how these synergistic signatures are not always present, and can be overshadowed by other emergent phenomena in the systems (*e.g.* the transition to the magnetized phase in the Ising model). Finally, we showed that a simple heuristical method that leveraged these signatures was able to detect higher-order mechanisms in a simple setting, providing a basis for future more refined inference schemes. We expect our results to be relevant for any attempts at reconstruct-

ing [16, 30, 37, 38] and predicting [7, 39] complex interacting systems from signals, as well as for the ongoing discussion about the nature and importance of higher-order systems [40].

* robiglio.thomas@phd.ceu.edu

† maxime.lucas@centai.eu

‡ giovanni.petri@nulondon.ac.uk

- [1] U. Grenander and M. I. Miller, *Journal of the Royal Statistical Society: Series B (Methodological)* **56**, 549 (1994).
- [2] J. D. Sterman, *System Dynamics Review* **10**, 291 (1994).
- [3] S. V. Scarpino and G. Petri, *Nature communications* **10**, 898 (2019).
- [4] X. Han, Z. Shen, W.-X. Wang, and Z. Di, *Physical Review Letters* **114**, 028701 (2015).
- [5] T. Squartini, G. Caldarelli, G. Cimini, A. Gabrielli, and D. Garlaschelli, *Physics Reports* **757**, 1 (2018).
- [6] T. P. Peixoto, *Physical Review X* **8**, 041011 (2018).
- [7] B. Prasse and P. Van Mieghem, *Proceedings of the National Academy of Sciences* **119**, e2205517119 (2022).
- [8] A.-L. Barabási, *Nature Physics* **8**, 14 (2012).
- [9] T. P. Peixoto, *Physical Review Letters* **123**, 128301 (2019).
- [10] N. Voges, V. Lima, J. Hausmann, A. Brovelli, and D. Battaglia, *Journal of Neuroscience* **44**, 10.1523/JNEUROSCI.0157-23.2023 (2024).
- [11] O. M. Cliff, A. G. Bryant, J. T. Lizier, N. Tsuchiya, and B. D. Fulcher, *Nature Computational Science* **3**, 883 (2023).
- [12] E. Bianco-Martinez, N. Rubido, C. G. Antonopoulos, and M. Baptista, *Chaos* **26**, 043102 (2016).
- [13] F. Battiston, E. Amico, A. Barrat, G. Bianconi, G. Ferraz de Arruda, B. Franceschiello, I. Iacopini, S. Kéfi, V. Latora, Y. Moreno, *et al.*, *Nature Physics* **17**, 1093 (2021).
- [14] F. E. Rosas, P. A. Mediano, A. I. Luppi, T. F. Varley, J. T. Lizier, S. Stramaglia, H. J. Jensen, and D. Marinazzo, *Nature Physics* **18**, 476 (2022).
- [15] F. Battiston, G. Cencetti, I. Iacopini, V. Latora, M. Lucas, A. Patania, J.-G. Young, and G. Petri, *Physics Reports* **874**, 1 (2020).
- [16] A. Santoro, F. Battiston, G. Petri, and E. Amico, *Nature Physics* **19**, 221 (2023).
- [17] F. E. Rosas, P. A. Mediano, M. Gastpar, and H. J. Jensen, *Physical Review E* **100**, 032305 (2019).
- [18] T. F. Varley, O. Sporns, S. Schaffelhofer, H. Scherberger, and B. Dann, *Proceedings of the National Academy of Sciences* **120**, e2207677120 (2023).
- [19] M. Gatica, R. Cofré, P. A. Mediano, F. E. Rosas, P. Orio, I. Diez, S. P. Swinnen, and J. M. Cortes, *Brain connectivity* **11**, 734 (2021).
- [20] K. Huang, *Introduction to statistical physics* (CRC press, 2009).
- [21] S. N. Dorogovtsev, A. V. Goltsev, and J. F. Mendes, *Reviews of Modern Physics* **80**, 1275 (2008).
- [22] I. Iacopini, G. Petri, A. Barrat, and V. Latora, *Nature Communications* **10**, 2485 (2019).
- [23] S. Stramaglia, T. Scagliarini, B. C. Daniels, and D. Marinazzo, *Frontiers in Physiology* **11**, 595736 (2021).

- [24] P. L. Williams and R. D. Beer, Nonnegative decomposition of multivariate information (2010), [arXiv:1004.2515 \[cs.IT\]](#).
- [25] V. Griffith and C. Koch, in *Guided self-organization: inception* (Springer, 2014) pp. 159–190.
- [26] T. F. Varley, M. Pope, M. G. Puxeddu, J. Faskowitz, and O. Sporns, *Proceedings of the National Academy of Sciences* **120**, e2300888120 (2023).
- [27] T. Schreiber, *Physical Review Letters* **85**, 461 (2000).
- [28] D. Merlini, *Lettere al Nuovo Cimento* (1971-1985) **8**, 623 (1973).
- [29] J. Liu, Y. Qi, Z. Y. Meng, and L. Fu, *Physical Review B* **95**, 041101 (2017).
- [30] H. Wang, C. Ma, H.-S. Chen, Y.-C. Lai, and H.-F. Zhang, *Nature communications* **13**, 3043 (2022).
- [31] M. E. Newman and G. T. Barkema, *Monte Carlo methods in statistical physics* (Clarendon Press, 1999).
- [32] R. Pastor-Satorras, C. Castellano, P. Van Mieghem, and A. Vespignani, *Reviews of Modern Physics* **87**, 925 (2015).
- [33] Triplets of random nodes behave similarly to 3-cliques, moreover it is of interest to discriminate between true and spurious three-body couplings.
- [34] T. M. Cover, *Elements of information theory* (John Wiley & Sons, 1999).
- [35] The statistical distance is half of the L^1 distance between the two discrete distributions.
- [36] The Ising model on a Erdős–Rényi random graph is well described by the known results for the mean-field Ising model [21], which has critical temperature given by $T_{\text{cr.}}/J = q$ where q is the coordination number of the lattice. Fixing the temperature $T = 1$ and with $q = \langle k_1 \rangle$ in our Hamiltonian Eq. (3) we obtain the critical value of the pairwise coupling: $J_1^{\text{cr.}} = 1$.
- [37] S. Piaggese, A. Panisson, and G. Petri, in *Learning on Graphs Conference* (PMLR, 2022) pp. 55–1.
- [38] A. Levina, V. Priesemann, and J. Zierenberg, *Nature Reviews Physics* **4**, 770 (2022).
- [39] C. Murphy, V. Thibeault, A. Allard, and P. Desrosiers, Duality between predictability and reconstructability in complex systems (2023), [arXiv:2206.04000 \[cond-mat.stat-mech\]](#).
- [40] V. Thibeault, A. Allard, and P. Desrosiers, *Nature Physics* , 1 (2024).

Supplemental Material

I. INFORMATION THEORETIC MEASURES

In the following section we present the two information theoretic measures that are used in the main text to probe low and higher-order behaviors, namely transfer entropy and total dynamical O-information.

A. Transfer Entropy

The Transfer Entropy (TE) is an information-theoretic measure of the directed (time-asymmetric) information transfer between two random processes [S1]. Given two variables X and Y , the TE from X to Y is defined as the mutual information between the present of X and the future of Y , conditioned on the past of Y :

$$\mathcal{T}(X \rightarrow Y) = \mathcal{T}(X; Y) \equiv \mathcal{I}(X_t, Y_{t+1} | Y_t) = \mathcal{H}(X_t, Y_{t+1}) + \mathcal{H}(Y_t, Y_{t+1}) - \mathcal{H}(X_t, Y_{t+1}, Y_t) - \mathcal{H}(Y_t) \quad (\text{S1})$$

The definition of the TE is asymmetric to capture the directed influence of the past of one variable on the future of another. In the main text we use TE as a low-order counterpart to the total dynamical O-information that we use to probe higher-order behavior. As we wish to consider the total transfer entropy present in a group of three nodes we sum up all the possible source-target combinations of the three nodes states. Given three variables X_1 , X_2 , and X_3 this is given by:

$$\begin{aligned} \mathcal{T}^{\text{tot.}}(X_1, X_2, X_3) = & \mathcal{T}(X_1; X_2) + \mathcal{T}(X_2; X_1) + \mathcal{T}(X_1; X_3) + \\ & + \mathcal{T}(X_3; X_1) + \mathcal{T}(X_2; X_3) + \mathcal{T}(X_3; X_2) \end{aligned} \quad (\text{S2})$$

B. Total dynamical O-information

The partial information decomposition (PID) framework is a well-established approach to characterize the information-sharing interdependencies between a group of three or more variables [S2–S4]. Qualitatively, these relations can be of three types: redundant, synergistic, or unique. Consider three variables sharing information, X_1 , X_2 and X_3 . Information is said to be redundant if it is replicated over the variables (that is, recoverable from $X_1 \vee X_2 \vee X_3$), synergistic if it can only be recovered from their joint state ($X_1 \wedge X_2 \wedge X_3$), and unique if it can only be recovered from one variable and nowhere else.

In this framework, mutual information has been extended to groups of three or more variables by the so-called O-information (shorthand for “information about Organizational structure”) [S5], which on a vector of n random variables $\mathbf{X} = (X_1, \dots, X_n)$ is given by:

$$\Omega_n(\mathbf{X}) \equiv (n - 2)\mathcal{H}(\mathbf{X}) + \sum_{j=1}^n [\mathcal{H}(X_j) - \mathcal{H}(\mathbf{X}_{-j})], \quad (\text{S3})$$

where $\mathcal{H}(\cdot)$ is the Shannon entropy [S6] and $\mathbf{X}_{-j} = \mathbf{X} \setminus X_j$ (see [S5] for a detailed presentation of this metric’s properties). For our purposes, the relevant property of O-information is that it is a signed metric: $\Omega_n(\mathbf{X}) > 0$ indicates that information-sharing is dominated by redundancy, $\Omega_n(\mathbf{X}) < 0$ indicates that it is dominated by synergy, and $\Omega_n(\mathbf{X}) = 0$ indicates a balance between both.

Total Dynamical O-information. To generalize the O-information of multivariate time series from equal-time correlations to the time-lagged correlations, Stramaglia *et al.* proposed *dynamical* O-information $d\Omega$ [S7]. It is defined by (i) considering n random variables $\mathbf{X} = (X_1, \dots, X_n)$ on which we have defined the standard O-information, and (ii) adding a new random variable Y . In this way, the O-information of the joint state between set \mathbf{X} and the new variable Y becomes:

$$\Omega_{n+1}(\mathbf{X}, Y) = \Omega_n(\mathbf{X}) + \Delta_n \quad (\text{S4})$$

where:

$$\Delta_n = (1 - n)\mathcal{I}(Y; \mathbf{X}) + \sum_{j=1}^n \mathcal{I}(Y; \mathbf{X}_{-j}) \quad (\text{S5})$$

where $\mathcal{I}(\cdot; \cdot)$ is the canonical mutual information between two variables [S6]. The additional term in Δ_n quantifies the variation of the total O-information induced by the addition of Y , effectively measuring the informational character of the circuits linking Y to the variables in \mathbf{X} . In particular, if Δ_n is positive, Y receives mostly redundant information from the set of variables \mathbf{X} , whilst if Δ_n is negative, then the influence of \mathbf{X} on Y is dominated by synergistic effects. To remove potentially confounding shared information due to common history or input signals, the dynamical O-information is defined by conditioning Eqs. (S4)-(S5) on the history Y_0 of the target variable Y :

$$d\Omega_n(Y; \mathbf{X}) \equiv (1 - n)\mathcal{I}(Y; \mathbf{X}|Y_0) + \sum_{j=1}^n \mathcal{I}(Y; \mathbf{X}_{-j}|Y_0). \quad (\text{S6})$$

Here $Y_0(t) = (y(t), y(t-1), \dots, y(t-\tau+1))$ and $Y = Y(t) = y(t+1)$ are the samples of Y corresponding to what we consider the past and present of the variable and to its next instance, respectively. The parameter τ is the temporal horizon of the time series and can typically be set to a relevant time scale of the process.

To quantify the dynamical information within a group of n units, regardless of source-target assignments, we define the *total* (or symmetrized) dynamical O-information as:

$$d\Omega_n^{\text{tot.}}(\mathbf{X}) \equiv \sum_{j=1}^n d\Omega_{n-1}(X_j; \mathbf{X}_{-j}). \quad (\text{S7})$$

When considering a delay $\tau = 1$, as in our work, we can rewrite the dynamical O-information using the transfer entropy in the following way:

$$d\Omega_n(Y; \mathbf{X}) \equiv (1 - n)\mathcal{T}(Y; \mathbf{X}) + \sum_{j=1}^n \mathcal{T}(Y; \mathbf{X}_{-j}) \quad (\text{S8})$$

II. HIGHER-ORDER DYNAMICAL MODELS

A. Simplicial Ising model

Low-order Ising model. The Ising model is a mathematical model of ferromagnetisms in statistical physics [S8]. It was originally defined on lattices and later extended to complex networks. We consider the general case of the model being defined on a graph $\mathcal{G} = (V, E)$, with $N = |V|$ nodes. To each node $i \in V$ we associate a binary state variable $S^i \in \{\pm 1\}$, corresponding to the spin state of the node, which can either be up ($S^i = +1$) or down ($S^i = -1$). The global state of the system is controlled by the Hamiltonian:

$$H = - \sum_i h_i S^i - \sum_{\langle i, j \rangle} J_{ij} S^i S^j \quad (\text{S9})$$

where $\{h_i\}$ are the local magnetic fields and $\{J_{ij}\}$ are the magnetic couplings for the neighbouring nodes $\{\langle i, j \rangle\}$. A special case of Eq. (S9) that allows for an exact analytical treatment in one and two-dimensional systems and a simple mean-field formulation is obtained with no magnetic fields (*i.e.* $h_i = 0 \forall i \in V$) and a positive uniform magnetic coupling $J_{ij} = J \forall \langle i, j \rangle \in \mathcal{G}$ with $J > 0$. In this case, the Hamiltonian of the systems takes the form:

$$H = -J \sum_{\langle i, j \rangle} S^i S^j \quad (\text{S10})$$

The energy of the system described by Eq. (S10) is minimized when all spins are aligned. The order parameter of these Ising models is the magnetization:

$$m = \frac{1}{N} \sum_i S^i \quad (\text{S11})$$

This parameter takes values in the interval $[-1, +1]$. The system described by Eq. (S10) undergoes a second-order phase transition between a fully disordered state ($m = 0$) and magnetized state ($|m| = 1$) at a critical value of the temperature T .

Extension to higher-order. The extension of the Ising model to incorporate many-body interactions is not a recent question in statistical physics [S9–S11]. Notably, so-called *plaquette* interactions involving groups of 4, 8, 16, *etc.* nodes appear when performing real-space renormalization on a square lattice, and higher-order terms appear when performing other renormalization procedures [S12]. Recently, a direct extension of Eq. (S10) has been proposed to describe an Ising model on a simplicial complex of order $\ell = 2$ [S13]. This model has a Hamiltonian given by:

$$H = -J_0 \sum_{\langle i,j \rangle} S^i S^j - J_1 \sum_{\langle i,j,k \rangle} S^i S^j S^k \quad (\text{S12})$$

where J_1 and J_2 are the strengths of two-body and three-body interactions, and $\langle i,j \rangle$ and $\langle i,j,k \rangle$ denote the two-body and the three-body connections in the 2-simplicial complex, respectively. However, as was already noted in the first analysis of the Ising model with three-body interactions, the extension provided by Eq. (S12) breaks the parity symmetry under spin flip at all sites of the dyadic model without magnetic field [S10]. This can be easily understood considering the energy of systems constituted by three spins S^1 , S^2 , and S^3 connected in a 2-simplex. There are two states with all spins aligned: all spins pointing up and all spins pointing down. These two configurations are symmetric upon flipping all spins, yet their energies when computed using Eq. (S12) are different, favoring the state with spins pointing up. To preserve the symmetry of the original low-order Ising model we propose an alternative formulation of the extension of the Ising model to simplicial complexes of arbitrary order. For every simplex σ —of all orders—we consider its only configuration favored in energy to be the one with all the spins aligned. This leads to formulating a new Hamiltonian for the simplicial Ising model:

$$H = -J_0 \sum_{i=1}^N S^i - \sum_{\ell=1}^{\ell_{\max}} J_\ell \sum_{\{\sigma \in \mathcal{K}: |\sigma|=\ell\}} \left[2 \bigotimes_{i \in \sigma} S^i - 1 \right] \quad (\text{S13})$$

where:

$$\bigotimes_{i=1}^n S^i = \delta(S^1, \dots, S^n) = \begin{cases} 1 & \text{if } S^1 = S^2 = \dots = S^n \\ 0 & \text{otherwise} \end{cases} \quad (\text{S14})$$

is the Kronecker delta with an arbitrary number of binary arguments and ℓ_{\max} is the maximal order of \mathcal{K} . For $\ell_{\max} = 1$ Eq. (S13) reduces to the low-order model with uniform magnetic field J_0 and pairwise coupling J_1 . Upon rescaling the couplings by the corresponding generalized degrees, we obtain the Hamiltonian used in our work.

Montecarlo dynamics. We consider the dynamics of this system to be the Markov chain of Monte Carlo moves performed with Metropolis-Hastings acceptance-rejection rule [S14] at temperature T . Monte Carlo dynamics are not defined to be dynamical models but rather numerical methods for solving statistical physics problems. However, the Metropolis-Hastings acceptance-rejection rule defines Markovian transitions between configurations of the model which we consider—to our scope—to be the dynamic of the system. We start from a random configuration in which each spin has equal probability of being in one of the two states. At each time step t we randomly select a set of independent spins (*i.e.* sites in the simplicial complex \mathcal{K} that are not first-neighbors). For each selected spin we propose a flipping move. In the case considered in the main text—simplicial complex with $\ell_{\max} = 2$ and no magnetic field, $J_0 = 0$ —the energy variation given by the flipping of spin i is given by:

$$\Delta E^i(t) = 2 \frac{J_1}{\langle k_1 \rangle} \sum_{j \in \partial_i} [2\delta(S^i(t), S^j(t)) - 1] + 2 \frac{J_2}{\langle k_2 \rangle} \sum_{(j,k) \in \nabla_i} [2\delta(S^i(t), S^j(t), S^k(t)) - 1] \delta(S^j(t), S^k(t)) \quad (\text{S15})$$

where ∂_i is the set of nodes in \mathcal{K} connected to node i by an edge and ∇_i is the set of pairs of nodes in \mathcal{K} forming a 2-simplex with node i . The acceptance or rejection of the proposed move is based on the Metropolis-Hastings rule, with the acceptance probability given by:

$$P(S^i(t) \rightarrow -S^i(t)) = \begin{cases} \exp\left[-\frac{\Delta E^i(t)}{T}\right] & \text{if } \Delta E^i(t) > 0 \\ 1 & \text{otherwise} \end{cases} \quad (\text{S16})$$

In other words, if we select a new state which has an energy lower than or equal to the present one, we should always accept the transition to that state.

B. Simplicial contagion model

The simplicial contagion model [S15] is a dynamical model defined to describe social contagion processes such as opinion formation or the adoption of novelties, where complex mechanisms of influence and reinforcement are at work. The model is defined on a simplicial complex \mathcal{K} with N nodes. In this models, the standard susceptible-infected-susceptible (SIS) compartmental model for contagion processes [S16] is extended to account for group interactions. Following the SIS framework [S17], to each node of a simplicial complex \mathcal{K} we associate a binary random variable $x_i(t) \in \{0, 1\}$ such that at each time step we divide the population of individuals into two classes of susceptible (S) and infectious (I) nodes, corresponding respectively to the values 0 and 1 of the state variables $x_i(t)$. At the initial time step a finite fraction of infected agents ρ_0 is placed in the population. At each time step, each susceptible agent ($x_i(t) = 0$) becomes infected with a probability β_ℓ if it belongs to a ℓ -simplex where all the other ℓ nodes are infected. The infected agents recover independently with probability μ . The order parameter of this model is the density of infected agents at time t , given by:

$$\rho(t) = \frac{1}{N} \sum_i x_i(t) \quad (\text{S17})$$

Rescaled infectivity rates. In the original paper [S15], the author provide an analytical characterization of the mean-field description of this model on simplicial complexes with $\ell_{\max} = 2$. Given the set of infection probabilities $\{\beta_\ell\}$ and the recovery rate μ , assuming homogeneous mixing and the independence between the states of different nodes, the mean-field expression for the temporal evolution of the density of infected nodes $\rho(t)$ is:

$$\dot{\rho}(t) = -\mu\rho(t) + \sum_{\ell=1}^{\ell_{\max}} \beta_\ell \langle k_\ell \rangle \rho^\ell(t) [1 - \rho(t)] \quad (\text{S18})$$

This expression can be simplified and treated analytically by rescaling time by a factor μ and introducing the rescaled infectivity rates $\{\lambda_\ell = \mu\beta_\ell / \langle k_\ell \rangle\}$. These rescaled infectivity rates are the control parameters we consider in our work.

III. NUMERICAL VALUES OF THE TOTAL DYNAMICAL O-INFO

In the main text we focus on the statistical distance between the distributions of the total dynamical O-info of 2-simplices and 3-cliques. In Fig. S1a,b we show in the numerical values of $d\Omega_3^{\text{tot}}$ in the parameter space. For additional reference we also show in Fig. S1c,d the numerical values of the order parameter of the two models (see Eq. (S11) and Eq. (S17)). In the Ising model (Fig. S1a,c), we see that in the phase in which the system is not magnetized the all groups of three nodes (2-simplices, 3-cliques and random triplets) behave synergistically, with the 2-simplices showing more negative values of $d\Omega_3^{\text{tot}}$. As the system magnetizes—this is particularly evident above the threshold of the pairwise model—information is duplicated across units of the system and thus the groups of nodes share redundant information, $d\Omega_3^{\text{tot}} \geq 0$. In the simplicial contagion model (Fig. S1b,d), we see that overall the groups of three nodes in the system behave synergistically with the 2-simplices always displaying more negative values of $d\Omega_3^{\text{tot}}$ with respect to the other groups of three nodes. The reason for which in the simplicial contagion model groups don't behave redundantly—as instead happens in the Ising model—when the order parameter is large (*i.e.* in the endemic phase of the contagion model) is due to the fact that infected nodes recover independently one from the other and independently from the global state of the system. For this reason, even in the endemic phase, the state of nodes is not frozen as happens in the magnetized phase of the Ising model and thus the synergistic behavior dominates over the redundant contribution and the $d\Omega_3^{\text{tot}}$ remains negative.

We can explicitly see the non-linearity of the relation between higher-order behaviors and higher-order mechanisms—mentioned in the main text when looking at the dependency of the detection accuracy on the strength of the parameters controlling the group interactions—in Fig. S2. In the figure we show the dependence of the total dynamical O-information of 2-simplices and the strenght of the parameters controlling the group interactions (J_2 and λ_2 respectively). The jump we see in the Ising model for $J_1 = 0.67$ is due to the transition to the magnetized phase that results in a redundancy-dominated interdependency between the units of 2-simplices.

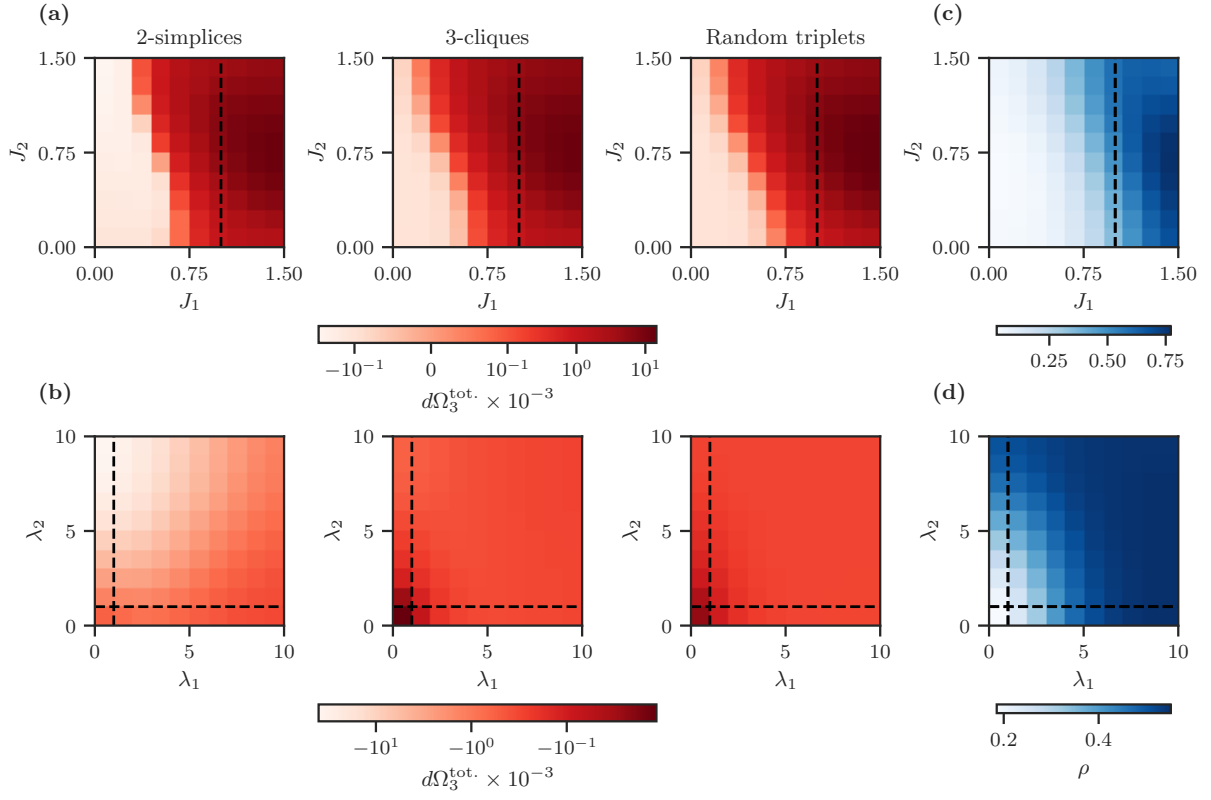


FIG. S1. (a)-(b) Numerical values of the $d\Omega_3^{\text{tot.}}$. (c)-(d) Order parameters (magnetization and density of infected agents). (a) Ising model. Results are obtained on a random simplicial complex with $N = 200$ nodes and average degrees $\langle k_1 \rangle = 20$, $\langle k_2 \rangle = 6$, running the Montecarlo dynamics for 3×10^4 time steps with $J_0 = 0$ at temperature $T = 1$. The dashed line is the critical coupling strength of the pairwise model $J_1^{\text{cr.}} = 1$ with no magnetic field. (b) Simplicial contagion model. Results are obtained on a random simplicial complex with $N = 200$ nodes and average degrees $\langle k_1 \rangle = 20$, $\langle k_2 \rangle = 6$, running the contagion dynamic for 10^4 time steps with $\mu = 0.8$ and $\rho_0 = 0.3$. The two dashed lines are respectively the epidemic threshold of the pairwise SIS model $\lambda_1^{\text{cr.}} = 1$ and the critical value of the rescaled 2-simplices infectivity rate above which the system shows the discontinuous phase transition and bistability $\lambda_2^{\text{cr.}} = 1$.

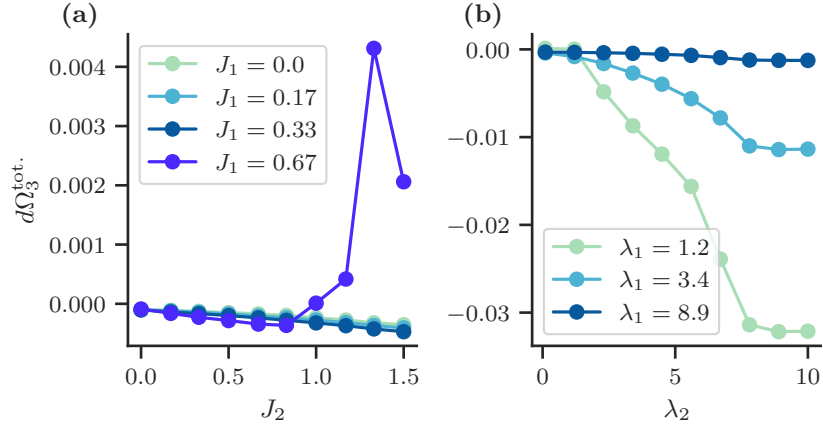


FIG. S2. Non-linearity of the relation between the total dynamical O-information of 2-simplices and the strenght of the parameters controlling the group interactions (J_2 and λ_2 respectively). (a) Ising model. (b) Simplicial contagion model.

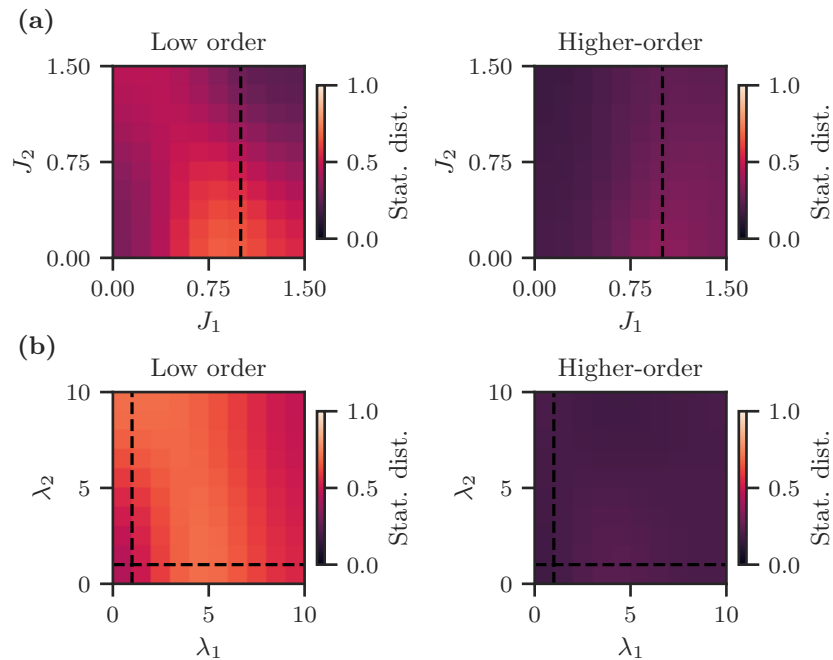


FIG. S3. **Statistical distance between the distributions of low (sum of transfer entropies) and higher-order (total dynamical O-information) observables of behavior of 3-cliques and random triplets.** (a) Ising model. (b) Simplicial contagion model.

IV. DIFFERENCES BETWEEN THE BEHAVIOR OF 3-CLIQUEs AND RANDOM TRIPLETS

In the main text we focus mainly on the difference measured by the information-theoretical metrics for behavior between 2-simplices and 3-cliques. In Fig. S3 we show the statistical distance between the distributions of low and higher-order observables of behavior between 3-cliques and random triplets (*i.e.* groups of three nodes not connected by a 2-simplex or a 3-clique). We see that overall the sum of transfer entropies provide a better discrimination between 2-cliques and random triplets with respect to total dynamical information. This is a conforing result for two reasons: (i) low order observables provide some discrimination between the interactions in the system and random group of nodes and (ii) as observed in the main text from the higher-order point of view 3-cliques and random triplets show similar behaviors. In the Ising model (panel a) we see that the statistical distance for the low order observables is larger in the vicinity of the critical point of the pairwise system. This echoes know results about the inverse Ising problem on graphs allowing for solutions based on mean-field inverse correlations near the critical point [S18]. In the simplicial contagion model (panel b) the statistical distance between the sum of transfer entropies in 3-cliques and random triplets is large in the majority of the space of the parameters. There are two regions in which the statistical distance is slightly smaller: for small values of both λ_1 and λ_2 (bottom left corner) and for large values of both the parameters. The reduced statistical distance in these two regions can be understood considering the dynamic of the system. When λ_1 and λ_2 are small the number of infected agents in the system is small or null, thus the state of nodes does not change much in time and we see no difference between interacting and disconnected nodes. Likewise, when $\lambda_1, \lambda_2 \gg 1$ the majority of the nodes are infected and thus also the states of non-interacting nodes are more correlated.

V. RANDOM CHOICE ACCURACY IN THE DETECTION OF HIGHER-ORDER INTERACTIONS

The random choice accuracy score in our detection method is given by the ratio between n_Δ and the number of 3-cliques in the skeleton of the simplicial complex under study. The nominator of this ratio is computed using the generalized degree as:

$$n_{\Delta} = \frac{N \times \langle k_2 \rangle}{3} \quad (\text{S19})$$

In the systems used for our results, the denominator in the accuracy ratio can be easily computed, as the skeleton of a random simplicial complex is an Erdős–Rényi (ER) random graph. The number of 3-cliques in a ER random graph with N nodes and edge probability p (and average degree $\langle k_1 \rangle = \langle k \rangle = p(N - 1)$) is given by:

$$\mathbb{E}_{N,p}[\# \text{ of 3-cliques}] = \binom{N}{3} p^3 = \frac{N(N-2)\langle k \rangle^3}{6(N-1)^2} \quad (\text{S20})$$

Using the parameters employed in our simulations ($N = 200$, $\langle k_1 \rangle = 20$, and $\langle k_2 \rangle = 6$), taking the ratio between Eq. (S19) and Eq. (S20) we obtain a random choice accuracy of 0.3.

-
- [S1] T. Schreiber, *Physical review letters* **85**, 461 (2000).
[S2] P. L. Williams and R. D. Beer, Nonnegative decomposition of multivariate information (2010), [arXiv:1004.2515 \[cs.IT\]](https://arxiv.org/abs/1004.2515).
[S3] V. Griffith and C. Koch, in *Guided self-organization: inception* (Springer, 2014) pp. 159–190.
[S4] T. F. Varley, M. Pope, null, null, and O. Sporns, *Proceedings of the National Academy of Sciences* **120**, [10.1073/pnas.2300888120](https://doi.org/10.1073/pnas.2300888120) (2023).
[S5] F. E. Rosas, P. A. Mediano, M. Gastpar, and H. J. Jensen, *Physical Review E* **100**, 032305 (2019).
[S6] T. M. Cover, *Elements of information theory* (John Wiley & Sons, 1999).
[S7] S. Stramaglia, T. Scagliarini, B. C. Daniels, and D. Marinazzo, *Frontiers in Physiology* **11**, 595736 (2021).
[S8] K. Huang, *Introduction to statistical physics* (CRC press, 2009).
[S9] R. Baxter and F. Wu, *Physical Review Letters* **31**, 1294 (1973).
[S10] D. Merlini, *Lettere al Nuovo Cimento* (1971-1985) **8**, 623 (1973).
[S11] T. R. Kirkpatrick and D. Thirumalai, *Physical review letters* **58**, 2091 (1987).
[S12] N. Goldenfeld, *Lectures on phase transitions and the renormalization group* (CRC Press, 2018).
[S13] H. Wang, C. Ma, H.-S. Chen, Y.-C. Lai, and H.-F. Zhang, *Nature communications* **13**, 3043 (2022).
[S14] M. E. Newman and G. T. Barkema, *Monte Carlo methods in statistical physics* (Clarendon Press, 1999).
[S15] I. Iacopini, G. Petri, A. Barrat, and V. Latora, *Nature communications* **10**, 2485 (2019).
[S16] A. Vespignani, *Nature physics* **8**, 32 (2012).
[S17] R. Pastor-Satorras, C. Castellano, P. Van Mieghem, and A. Vespignani, *Reviews of modern physics* **87**, 925 (2015).
[S18] H. C. Nguyen, R. Zecchina, and J. Berg, *Advances in Physics* **66**, 197 (2017).